FRAGMENTATION OF METHYL NITRITE BY PHOTON EXCITATION AND ENERGY TRANSFER FROM METASTABLE RARE GAS ATOMS

F. LAHMANI, C. LARDEUX and D. SOLGADI

Laboratoire de Photophysique Moléculaire, Laboratoire associé à l'Université Paris-Sud, Bâtiment 213, Université Paris-Sud, 91405 Orsay (France)

(Received November 11, 1982; in revised form February 8, 1983)

Summary

The fluorescence of electronically excited NO resulting from the fragmentation of CH_3ONO either by photons of energy 8.43 and 10.03 eV (xenon and krypton resonance lines) or by collisional energy transfer from Xe $^3P_2$ and Kr $^3P_{0,2}$ was studied under identical pressure and detection conditions. The electronic branching ratios (NO A)/(NO B) for the two modes of excitation are different. In the photolysis NO($A\ ^2\Sigma^+ - X\ ^2\Pi$) emission dominates while NO($B\ ^2\Pi - X\ ^2\Pi$) bands appear in the presence of added argon. At 10.03 eV NO C $^2\Pi$ ($v' = 0$) and D $^2\Sigma^+$ ($v' = 0$) are also produced. For the dissociative excitation by metastable rare gas atoms the relative formation of NO B is higher than that observed in the photodissociation. The NO A vibrational populations are similar for both modes of excitation, indicating that the same dissociative state may be involved. For Xe $^3P_2$ and Kr $^3P_{0,2}$ reactive quenching, the NO B vibrational population decreases exponentially with v' and is slightly higher than the distribution calculated on the basis of statistical energy partitioning.

1. Introduction

In the fragmentation of an energy-rich polyatomic molecule the energy available after the bond has broken must be partitioned between the translation and the rovibronic degrees of freedom of the products. If one of the fragments is electronically excited its vibrational and rotational energy content can be directly determined from the emission spectrum, and thus the study of fragment fluorescence before subsequent collisional deactivation provides a useful and simple method of probing the distribution of energy states in the dissociation products. In the dissociation of large polyatomic molecules at high energy, it is generally assumed that the energy is rapidly randomized in the dense manifold of levels and if there is no barrier in the exit channel a statistical distribution of the excess energy among the degrees of freedom of the product will be observed. The dominant parameter is then the energy. To test this hypothesis, the energy of the activated molecule

0047-2670/83/$3.00

TABLE 1

Energies of excited states of heavy rare gas atoms

Atom	*E* (eV) *for the following states*			
	$^1P_1$	$^3P_0$	$^3P_1$	$^3P_2$
Ar	11.83	11.7	11.62	10.5
Kr	10.64	10.5	10.03	9.90
Xe	9.57	9.4	8.43	8.3

must be controlled and defined. Two different selective modes of preparation of the dissociating molecule can be used: direct photon excitation or collision with metastable species. More precisely, for the large energy input that is generally required to produce electronically excited fragments, it is interesting to compare the results of direct photolysis experiments using rare gas resonance lines as the source of vacuum UV photons with the results of collisional energy transfer from Ar $^3P_{0,2}$, Kr $^3P_{0,2}$ and Xe $^3P_{0,2}$. The various excited states of the rare gas atoms have very similar energies as reported in Table 1.

The product distribution in vacuum UV photodissociation and dissociative excitation using metastable rare gas atoms has already been examined in a few cases such as HCN [1] and H_2O [2]. The vibrational and rotational populations of CN B $^2\Pi$ and OH A $^2\Sigma^+$ show the same trends for both modes of excitation. However, valuable comparisons are not easy to make since the experiments reported do not always involve similar excess energies and have not been performed under identical pressure and detection conditions. Moreover, analysis of collisional excitation using metastable atoms is complicated by the fact that some of the excess energy is converted into the translational energy of the incident atom.

In this work we have undertaken a comparative study of the fluorescence of NO resulting from the fragmentation of CH_3ONO excited either using xenon and krypton resonance lamps at 147 and 123.6 nm or by collisional energy transfer from metastable xenon and krypton atoms.

The primary photochemical reaction in organic nitrites is the rupture of the RO—NO bond (D_0^0 = 1.8 eV) [3]. In the vacuum UV the energy deposited in the molecule far above the dissociation energy is sufficient to allow the production of an electronically excited fragment. In fact, the photodissociation of organic nitrites at 123.6 nm (10.03 eV) and 147 nm (8.43 eV) has previously been shown to give rise to electronically excited NO which fluoresces [4]. In previous work [5] we have performed a detailed study of the excitation energy dependence of the formation of excited NO from CH_3ONO in the range 115 - 165 nm using synchrotron radiation as a tunable photon source in the vacuum UV region. The excitation spectra of individual vibronic states of NO show that NO A $^2\Sigma^+$ (v' = 0, 1, 2, 3) is the main fluorescent species between 160 and 140 nm while between 135 and 115 nm NO

C $^2\Pi$ ($v' = 0$) and NO D $^2\Sigma^+$ ($v' = 0$) are formed together with the A $^2\Sigma^+$ state. It should be noted that only Rydberg states have been observed. The valence state NO B $^2\Pi$, although energetically allowed, was not detected under these experimental conditions. The relative vibrational population of NO A ($v' = 0, 1, 2, 3$) has been determined as a function of the excess energy and can be explained on the basis of a statistical energy partition between CH_3O and NO if CH_3O is assumed to behave as a triatomic radical (only three modes of vibration are activated in the dissociation process).

It is of interest to perform a parallel investigation of the photofragment fluorescence resulting from dissociation induced by energy transfer to determine whether the same dissociative pattern is obtained for different methods of excitation. The statistical behaviour of the vibrational energy disposal for a polyatomic molecule with a large density of states such as CH_3ONO would be expected to be independent of the mode of preparation of the dissociative state. However, it is important to determine whether the same selectivity (only Rydberg states were populated in photon excitation) was observed in excitation by metastable rare gas atoms.

2. Experimental details

The radiation sources were flow discharge atomic resonance lamps built according to the method of Davies and Braun [6]. The discharged gases were xenon (3% in helium) which provided the 147 nm resonance line and krypton (4% in helium) which provided the 123.6 nm line. The power source was a 2450 MHz microwave power generator operated using a Broida-type cavity. The flow rate was adjusted to obtain the highest intensity (150 cm^3 min^{-1}). The fluorescence cell was directly attached to the discharge lamp and was separated from it by an MgF_2 window (Fig. 1). The emission was observed at right angles to the incident beam and was focused on the slit of a 0.6 m Jobin–Yvon HRS monochromator equipped with a grating (1200 grooves mm^{-1}) blazed at 250 nm. The signal intensity was detected using a

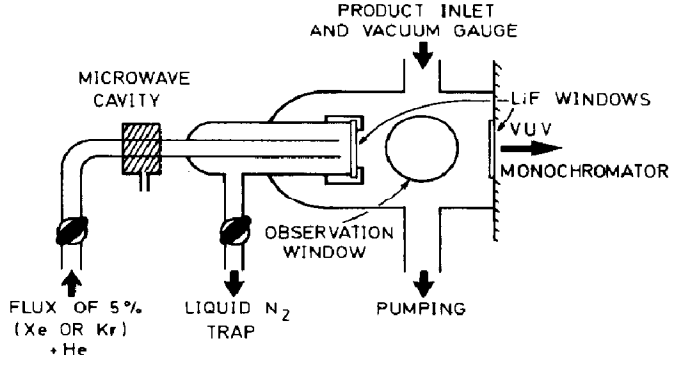

Fig. 1. Schematic diagram of the rare gas lamp and the fluorescence cell for the photolysis experiments.

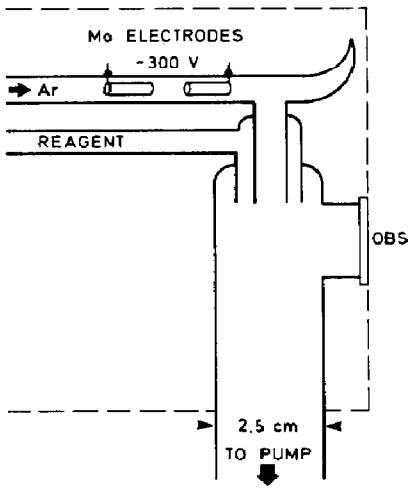

Fig. 2. Schematic diagram of the flowing afterglow apparatus for dissociative excitation using metastable rare gases.

cooled EMI 9635 Q or 6256 S photomultiplier and a conventional photon counting device. Because of its rapid decomposition a continuous flow of the reactant through the cell was maintained.

A flowing afterglow system similar to that described by Koltz and Setser [7] was used for the metastable rare gas energy transfer experiments. A schematic diagram of the apparatus is shown in Fig. 2. Metastable xenon and krypton atoms were generated by adding a small amount of xenon or krypton to the main argon flow through a pair of rolled molybdenum foil electrodes operated at 200 - 300 V. The flow reactor was pumped using a mechanical pump at a rate of 60 $m^3\ h^{-1}$. The mixing zone, which was 7 cm downstream of the electrodes, had a coaxial geometry. The rare gas flowed through the inner tube (inside diameter, 6 mm) and the reactant was introduced through the outer tube. The discharge was separated from the mixing region by a 90° bend and a Wood's horn to eliminate the effects of resonance radiation. The pressure of argon in the flow reaction was maintained at about 2 Torr. The total quenching by xenon or krypton of the Ar $^3P_{0,2}$ initially present in the discharge was checked by noting the absence of $N_2(C \rightarrow B)$ emission on addition of nitrogen to the reaction zone. In theory both Xe $^3P_0$ and Xe $^3P_2$ should be present in the reaction zone; however, experimental evidence indicates that in this type of flowing afterglow system the Xe $^3P_0$ concentration is less than 0.1% of the $^3P_2$ concentration [8]. The fluorescence was observed through a Suprasil window using a 0.60 m Jobin–Yvon monochromator with the slit aligned parallel to the glas flow. The spectra were recorded using the same combination of photomultiplier and photon counting electronics as before and were displayed on a Zoomax SEIN multichannel analyser operating in the multiscale mode. In both cases the multichannel analyser was interfaced to a Tektronix 4051 computer for data acquisition and treatment.

The spectral response of the detection system was calibrated using a standard lamp with a known absolute output in the region 260 - 400 nm. The NO(A ($v' = 0$) → X (v'')) band intensities from CH_3ONO dissociation were compared with the known relative transition probability to calibrate the 220 - 300 nm region. The correction factor is obtained by dividing the measured intensities by the known Franck–Condon factors for the transition involved [9].

CH_3ONO was prepared by reacting sodium nitrite with methanol in a sulphuric acid medium. The samples were thoroughly degassed before use to remove any possible NO impurity. The sample pressures were measured using a Sogev Mediovac gauge which had previously been calibrated against a Baratron manometer (MKS).

3. Results

3.1. Photon excitation

A typical fluorescence spectrum from the photolysis of CH_3ONO at 147 nm is shown in Fig. 3. For pure CH_3ONO at $\lambda_{exc} = 147$ nm, the emission between 200 and 400 nm can be attributed almost exclusively to the NO($A\ ^2\Sigma^+ - X\ ^2\Pi$) transition (Fig. 3(a)). For the krypton lamp ($\lambda_{exc} = 123.6$ nm) the spectrum shows new features towards the shorter wavelength end which can be assigned to the NO(C ($v' = 0$)–X) and NO(D ($v' = 0$)–X) progressions. These assignments are in general agreement with earlier results [4] obtained using synchrotron radiation. However, the fluorescence in the 300 - 400 nm range reveals a broad low intensity rotational structure without any clear band heads which is difficult to identify. To obtain spectra recorded under similar conditions to those used in the metastable experiments, argon at 1 - 5 Torr was added to CH_3ONO. The emission (Fig. 3(b)) is modified and exhibits well-developed bands shaded towards the red which correspond to the NO(B ($v' = 0, 1, 2$)–X) transition. The branching ratio A/B and the populations of the vibrational levels of NO A and NO B were determined by integrating the fluorescence signals of given emission bands, taking into account the detection sensitivity, and dividing by the relative transition probability [9]

$$P_{v'v''} = \frac{q_{v'v''}\nu^3}{\Sigma q_{v'v''}\nu^3}$$

This calculation was performed for several pairs of bands because the overlap of some of them can introduce important errors. The results are reported in Table 2.

A band contour analysis was also performed for the NO(A ($v' = 0$)–X ($v'' = 1$)) emission band to obtain information on the rotational energy disposal in NO from CH_3ONO photolysis at low pressure (0.1 Torr). The recording of the 0–1 band at a resolution of 0.05 nm (Fig. 4) corresponds to the contour expected for a Boltzmann distribution of the rotational levels.

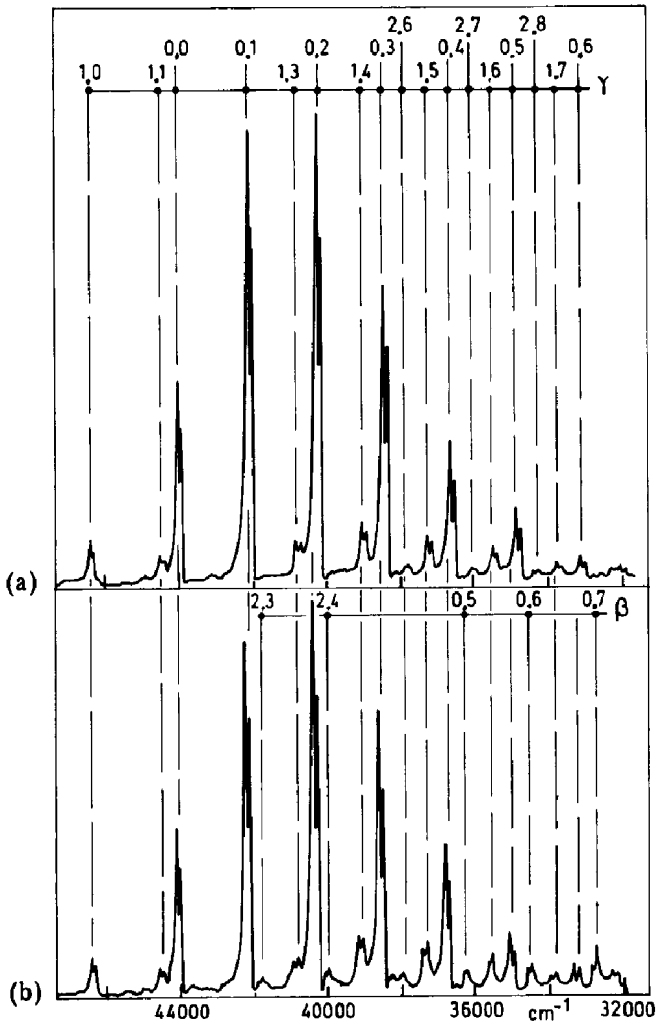

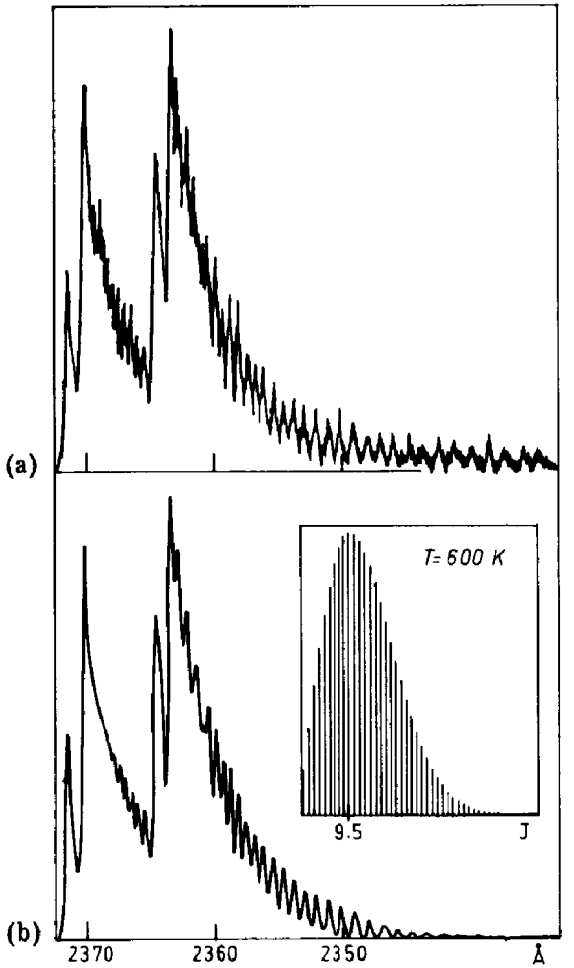

Fig. 3. Emission spectrum of NO from the photolysis of CH_3ONO at 147 nm: (a) $p(CH_3ONO)$ = 100 mTorr; (b) $p(CH_3ONO)$ = 100 mTorr + p(argon) = 5 Torr.

Fig. 4. (a) Experimental and (b) simulated spectra of the NO(A (v' = 0)–X (v' = 1)) band from the photolysis of CH_3ONO at 147 nm.

TABLE 2

Vibrational population and electronic branching ratio of NO A and NO B in the photodissociation of CH_3ONO

	λ_{exc} = 147 nm							λ_{exc} = 123.6 nm					
	NO A			NO B			B/A	NO A		NO B			B/A
	$v' = 0$	$v' = 1$	$v' = 2$	$v' = 0$	$v' = 1$	$v' = 2$		$v' = 0$	$v' = 1$	$v' = 0$	$v' = 1$	$v' = 2$	
CH_3ONO (100 mTorr)	1	0.26	0.081	Not detectable				1	0.37	Rotational excitation			
CH_3ONO (100 mTorr) + Ar (2 Torr)	1	0.30	0.085	1	0.71	0.61	0.12	1	0.46	1	0.83	0.82	0.30
CH_3ONO (100 mTorr) + Ar (5 Torr)	1	0.31	0.085	1	0.72	0.64	0.11	1	0.63	1	0.85	0.85	0.4

Because of the complexity of the band, which consists of 12 branches, the experimental spectrum was reproduced by computer simulation. For a given Boltzman temperature in the A $^2\Sigma^+$ state the program generates a fully resolved line spectrum using the line strength of Earls [10] and the spectroscopic constant of Engleman and Rouse [11]. The line spectrum is then convoluted using an empirical gaussian slit function corresponding to the experimental slit function and the calculated intensities are summed over each small frequency interval. Figure 4 shows the simulated spectrum which gives the best fit to the experimental data. The Boltzmann distribution used corresponds to a rotational temperature of 600 K.

For excitation at 123.6 nm no determination of the rotational energy was attempted because part of the NO A was produced directly and part was produced by radiative cascade from higher states.

3.2. *Dissociative excitation by metastable rare gas atoms*

The emission from the chemiluminescent reactions

$Xe\ ^3P_2 + CH_3ONO$

and

$Kr\ ^3P_{0,2} + CH_3ONO$

was investigated in the 200 - 400 nm spectral region. Typical spectra are shown in Fig. 5. The most intense features in the 190 - 300 nm range are still assigned to the NO(A $^2\Sigma^+$–X $^2\Pi$) transition. Above 300 nm the NO(B $^2\Pi$–X $^2\Pi$) system dominates because of favourable Franck–Condon factors. For

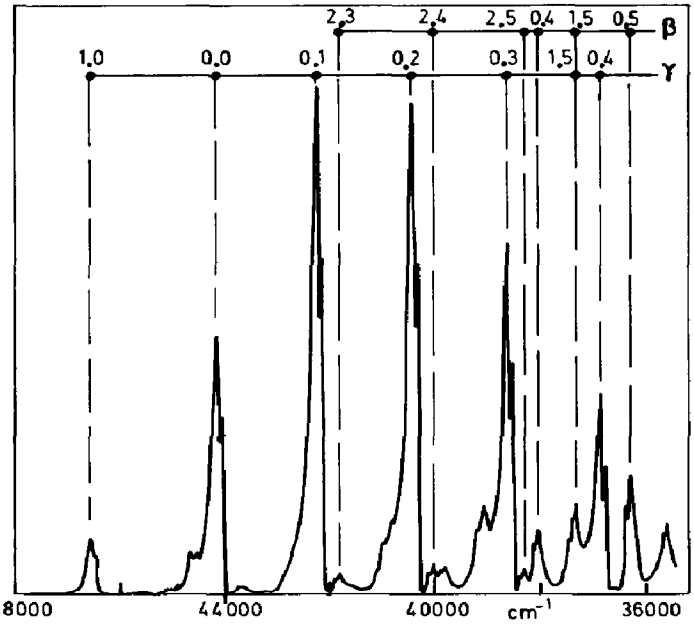

Fig. 5. Part of the fluorescence spectrum of NO from the reaction of CH_3ONO with Xe $^3P_2$.

Kr $^3P_{0,2}$ some new bands appear between 200 and 220 nm which can be attributed to NO C $^2\Pi$ ($v' = 0$) and NO D $^2\Sigma^+$ ($v' = 0$) states. Increasing the CH_3ONO pressure from 10 to 300 mTorr does not change the relative intensity of the vibronic bands within the A and B manifold but it does modify the branching ratio A/B. It has been shown before that the quenching rate constant of NO A $^2\Sigma^+$ does not depend on the vibrational level for $v' = 0, 1, 2, 3$; it is $k^A_{CH_3ONO} = (6.2 \pm 0.6) \times 10^{-10}$ cm^3 molecule^{-1} s^{-1}. The quenching rate constant of NO B by CH_3ONO is not known, but as the radiative lifetime of NO B (3 μs) is one order of magnitude larger than that of NO A (200 ns) it can be predicted that for a given pressure of CH_3ONO the B state will be more quenched than the A state which explains the increase in the branching ratio A/B with CH_3ONO pressure. The pressure effect on the relative A–B population has been used to determine the electronic branching ratio at the zero limit pressure and the quenching rate for NO B ($v' = 0$) by CH_3ONO. The application of the steady state principle to the kinetic scheme

$$\text{Xe } {}^3P_2 \text{ (or Kr } {}^3P_{0,2}) + CH_3ONO \begin{cases} \nearrow \text{NO A } (v' = 0) & k_A \\ \searrow \text{NO B } (v' = 0) & k_B \end{cases}$$

$$\text{NO A} \longrightarrow \text{NO X} + h\nu_F \qquad k^A_F$$

$$\text{NO A} + CH_3ONO \longrightarrow \text{NO X} \qquad k^A_{CH_3ONO}$$

$$\text{NO B} \longrightarrow \text{NO X} + h\nu_F \qquad k^B_F$$

$$\text{NO B} + CH_3ONO \longrightarrow \text{NO X} \qquad k^B_{CH_3ONO}$$

gives

$$I_F(\text{NO A}) \propto \frac{k^A_F}{k^A_{CH_3ONO}[CH_3ONO] + k^A_F} \frac{k_A}{k_A + k_B}$$

$$I_F(\text{NO B}) \propto \frac{k^B_F}{k^B_{CH_3ONO}[CH_3ONO] + k^B_F} \frac{k_B}{k_A + k_B}$$

$$\frac{I_F(\text{NO A})}{I_F(\text{NO B})} \propto \frac{k_A}{k_B} \frac{1}{1 + k^A_{CH_3ONO}\tau_A[CH_3ONO]} (1 + k^B_{CH_3ONO}\tau_B[CH_3ONO])$$

As $k^A_{CH_3ONO}$, τ_A ($= 2 \times 10^{-7}$ s) and τ_B ($= 3 \times 10^{-6}$ s) are known, the electronic branching ratio for the reactive quenching of Xe $^3P_2$ and Kr $^3P_{0,2}$ by CH_3ONO and $k^B_{CH_3ONO}$ can be deduced from the dependence of I_F(NO A)/I_F(NO B) on the CH_3ONO pressure:

$(k_A/k_B)_{Xe} = 2.2 \pm 0.1$

$(k_A/k_B)_{Kr} = 1.4 \pm 0.1$

$k^{B,v'=0}_{CH_3ONO} = 0.6 \pm 0.1 \times 10^{-10}$ cm^3 molecule^{-1} s^{-1}

TABLE 3

Vibrational populations and electronic branching ratios of NO A and NO B in metastable reactive quenching

	$Xe\ ^3P_2 + CH_3ONO$	$Kr\ ^3P_{0,2} + CH_3ONO$
NO A		
$v' = 0$	1	1
$v' = 1$	0.20	0.43
$v' = 2$	0.06	0.13
$v' = 3$	0.04	0.06
NO B		
$v' = 0$	1	1
$v' = 1$	0.25	0.36
$v' = 2$	0.14	0.30
$v' = 3$	0.06	0.20
$v' = 4$	0.02	0.15
$v' = 5$	0.01	0.096
$v' = 6$		0.055
$(B\ (v' = 0))/(A\ (v' = 0))$	0.45	0.72
B/A	0.48	1

The vibrational populations of NO A and NO B were determined as before by dividing the intensity of selected bands by the factor $q_{v'v''}\nu^3/\Sigma q_{v'v''}\nu^3$. The results are reported in Table 3. It is assumed that for NO B the electronic quenching is faster than the vibrational relaxation and does not depend on the v' level so that the NO B vibrational population is independent of the CH_3ONO pressure.

4. Discussion

The most important conclusions that can be drawn from the comparison of the experimental results are as follows.

(1) Under identical conditions of pressure, the electronic branching ratio between NO A and NO B differs for the two excitation modes, NO B formation being favoured in the reactive quenching of the metastable xenon and krypton atoms.

(2) Similar vibrational distributions in the A state are obtained in both excitation modes.

(3) In collision-induced fragmentation the relative vibrational population in NO B shows an exponential decrease with increasing v'.

We shall now discuss the implications of these results on the possible mechanisms of CH_3ONO fragmentation in the 7 - 10 eV region.

4.1. Electronic branching ratio

The electronic states of CH_3ONO have not been calculated in this energy region but a recent theoretical study of nitrous acid (HONO) [12] can be

used to predict the possible transitions in its methyl ester derivative. This calculation shows that Rydberg singlet and triplet states are located in the 7.4 - 9.7 eV region, while a π,π^*-type transition localized on the N=O double bond is situated at 10.2 eV for the singlet state and at 8.04 eV for the triplet state. Vacuum UV photodissociation has been shown previously to be quite selective in producing Rydberg states of NO, and the present work indicates that the valence state of NO B that is energetically allowed needs to be collisionally induced with both xenon and krypton resonance line irradiation. The effect of pressure on the appearance of NO B band heads can be interpreted in two different ways: either the NO B species is not formed in the primary process but results from collisional relaxation from another NO excited state, or NO B is produced in a highly non-Boltzmann rotational distribution and is relaxed by pressure to thermal equilibrium. The broad low intensity fine structure observed in the vicinity of the NO(B–X) emission at low CH_3ONO pressures appears to support the second possibility. It should be pointed out that the B/A branching ratio in a thermally equilibrated system increases from 0.11 at 147 nm to 0.4 at 123.6 nm. This increase may be due to a higher probability for excitation of the π,π^*-type transition in CH_3ONO at shorter wavelength which could correlate preferentially with the NO B $^2\Pi$ valence state.

Two mechanisms are involved in rare gas dissociative excitation: either a triplet–triplet energy transfer takes place or a collisional complex is formed. The triplet states of CH_3ONO that can be excited from Kr $^3P_{0,2}$ and Xe $^3P_2$ transfer are Rydberg triplet states of the same configuration as the singlet states involved in the absorption spectrum, but the triplet state localized on the N=O double bond can also be reached from Xe $^3P_0$ at lower energies as can be deduced from the calculations for HONO. The π,π^* transition in HONO is similar to the X $^2\Pi \rightarrow$ B $^2\Pi$ transition in pure NO, and it is probable that this electronic configuration can correlate with NO B at large CH_3O–NO separations. This may explain the formation of NO B in the energy transfer experiments. However, a charge transfer mechanism has often been postulated for the reactive quenching of metastable rare gases by halogen-containing molecules. If this route were involved with CH_3ONO, the crossing between the Xe $^3P_2$–CH_3ONO and Xe^+–CH_3ONO^- potential surfaces, which must occur at large distances, would produce by rapid electron transfer the negative ion CH_3ONO^- in the presence of Xe^+. The dissociative exit channels from this complex could differ from those observed in photodissociation because the change in the bond length in the ionic structure could favour NO B formation.

4.2. Vibrational energy partitioning

The vibrational distribution in the A state is not markedly different for the two modes of excitation, particularly at the lowest energy input (xenon lamp and Xe $^3P_2$ collisions) where no higher Rydberg states of NO can be produced. The slightly higher vibrational population obtained in the photolysis can be explained by the correspondingly larger energy available in this

latter case. This suggests that the same dissociative path leading to NO A is operative after both modes of preparation and that the excess energy available is the determining factor in the energy disposal. This indicates that excitation with metastable rare gases donates the entire available energy to CH_3ONO and that very little energy is lost in relative translation after the collision.

It is useful to compare the experimental population with an *a priori* distribution where it is assumed that all product quantum states allowed by energy conservation are equally probable. This assumption is based on unimolecular dissociation theory for a loose transition complex. It implies that (i) the dissociation is not direct, (ii) as a consequence of (i) the energy is rapidly randomized before the dissociation can occur and (iii) there is no dynamical effect during the recoil of the fragments. Such a treatment has previously been applied to a photon wavelength dependence study of the photodissociation of organic nitrites in the vacuum UV region [5]. The experimental populations are compared with a statistical calculation where the probability of forming NO A (v') is assumed to be proportional to the density of states given by

$$\rho(v',E) = \sum_{J=0}^{J_{max}} (2J+1) \int_0^{E-E_{v'}^{NO}-E_J^{NO}} \rho_I(E_I^{CH_3O})\rho_T \, dE_I$$

$\rho_T = E_T^{1/2}$ is the translational density of states and $E_T = E - E_{v'}^{NO} - E_J^{NO} - E_I^{CH_3O}$ is the relative translational energy of the products. The vibrational–rotational density of states $\rho_I(E_I^{CH_3O})$ of CH_3O has been computed as a function of the energy E [5]. It is assumed that the total available energy

$$E = E^*(\text{Xe (or Kr) } {}^3P_{0,2}) - D_0(CH_3ONO) - E(\text{NO A})$$

is released in the product degrees of freedom. The experimental and calculated populations are shown in Table 4.

In the quenching of the metastable rare gas, as in the photodissociation experiments, the NO A fragment is more vibrationally excited than predicted by the total equilibration of energy.

TABLE 4

Comparison of the experimental and the statistically predicted vibrational population for NO A produced by the photofragmentation of CH_3ONO at 147 nm or by the Xe $^3P_2$ reaction

v'	*147 nm*			*Xe* $^3P_2$		
	ΔE (cm^{-1})	P_{obs}	P_{calc}	ΔE (cm^{-1})	P_{obs}	P_{calc}
0	9200	0.75	0.906	8136	0.77	0.913
1	6890	0.19	0.090	5730	0.153	0.082
2	4620	0.06	0.004	3794	0.046	0.003
3				1196	0.030	10^{-4}

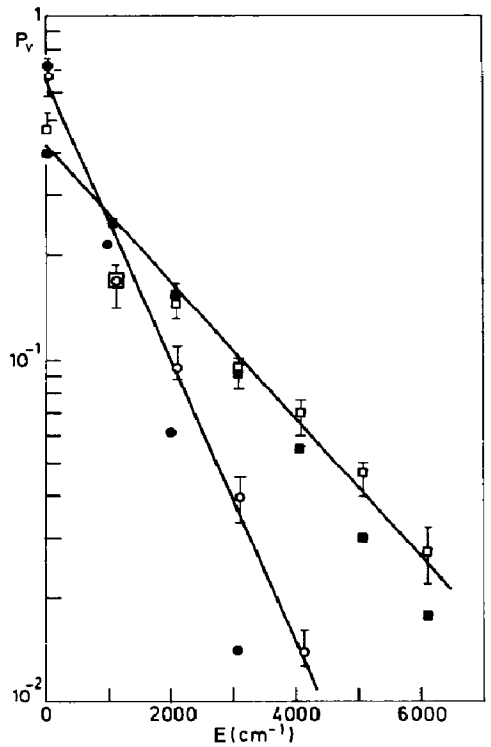

Fig. 6. NO B vibrational population produced in the dissociative excitation of CH_3ONO by Xe $^3P_2$ (○, observed; ●, calculated) and Kr $^3P_{0,2}$ (□, observed; ■, calculated).

The relative vibrational energy population produced in the NO B fragment by collisional excitation with metastable rare gases approximates a Boltzmann behaviour as shown by the linear semilogarithmic plot in Fig. 6. However, there is a deviation which is greater than the error limit for the two first vibrational levels: the $v' = 0$ level is slightly overpopulated and the $v' = 1$ level is slightly underpopulated relative to the exponential distribution of the highest levels. In view of this observation, it is necessary to ensure that the initial population has not been modified by collisional phenomena. NO B has a larger radiative lifetime (3 μs) than NO A (200 ns), and the pressure in the afterglow system (rare gas at about 2 Torr and CH_3ONO at about 30 - 100 mTorr) allows NO B to undergo about 60 collisions with argon and one to three collisions with CH_3ONO during its lifetime. The rate constant for one-step vibrational relaxation by argon is not known for NO B but has been shown to be 10^{-4} times the collision rate for NO A [13] and two orders of magnitude less for NO X [14]. It seems that this process can be ruled out for the vibrational deactivation of NO B in the present case. However, a non-direct relaxation mechanism involving a pressure-induced crossing to the closely lying b $^4\Sigma^-$ manifold followed by inverse electronic crossing to a lower vibrational state of NO B has been suggested to explain the relative vibrational population obtained in N–O recombination [15]. Such a process

should be faster for NO B ($v' > 3$) which has a resonance close to the vibrational levels of the b quartet state.

Electronic quenching by CH_3ONO has been evaluated in this work to be one-fifth of the gas kinetic rate constant for B ($v' = 0$) but has not been examined for higher v'. The quenching parameters of NO B vibrational states by CO_2, O_2, N_2O and H_2O [16] have been shown to be lower for $v' = 1$ and $v' = 2$ than for $v' = 0$ and $v' = 3$. If this were the case for CH_3ONO it would give an opposite effect to that observed here. In the absence of further information on the deactivation path in NO B vibrational states and because of its relatively small importance the observed anomaly will be neglected.

The vibrational temperatures of NO B due to excitation by Xe $^3P_2$ and Kr $^3P_{0,2}$ are calculated to be 1500 K and 3100 K respectively from the slopes of the linear plots in Fig. 6. The calculated statistical populations expected if total energy randomization is assumed are also shown in Fig. 6. The experimental points indicate a vibrational temperature rather higher than that predicted by the statistical calculation. It thus appears that for NO B the proportion of the excess energy being transformed into vibration, although approximating the exponential distribution expected in the statistical assumption for a long-lived complex, is not totally randomized. It should be mentioned as stated before that deviations from the statistical distribution in the products of the fragmentation of a polyatomic molecule as observed in the present work can be interpreted as resulting from incomplete energy randomization only when there is no energy barrier in the exit channel. There are no data on CH_3O X–NO A or CH_3O X–NO B potential surfaces but it is known that the recombination reactions of ground state radicals proceed with a zero activation energy. It thus seems more likely that the greater internal excitation of the NO product can be attributed to the reaction mechanism for both activation methods: a rapid predissociation occurs on a time scale of the same order of magnitude as the intramolecular vibrational relaxation.

5. Conclusion

In this work we have studied the fluorescence from excited NO resulting from the fragmentation of CH_3ONO at Xe $^3P_1$, Xe $^3P_{0,2}$, Kr $^3P_1$ and Kr $^3P_{0,2}$ energies. We have determined the electronic branching ratio and the vibrational distribution following the dissociation induced by photons emitted by rare gas resonance lamps or by collisional energy transfer from the metastable states of the same atoms in a flowing afterglow. More NO B was formed by metastable atom excitation than by the photodissociation reaction which suggests a specific dissociative mechanism in this case. The extent of vibrational excitation of NO A is similar for both modes of excitation. This can be interpreted by assuming that the formation of excited NO A follows a common channel regardless of the manner in which the energy is deposited in the CH_3ONO molecule. This result also indicates that all the energy available in the metastable atom is transferred to CH_3ONO. The NO A and NO B

vibrational populations were compared with statistical calculations performed assuming total energy randomization. Although the distributions are not completely equilibrated, the comparison suggests that a statistical assumption for the distribution of excess energy available in the reaction can explain the energy partitioning observed in this high energy polyatomic fragmentation.

References

1 A. Mele and H. Okabe, *J. Chem. Phys., 51* (1969) 4798.
T. Ursu and K. Kuchitsu, *Chem. Phys. Lett., 18* (1973) 337.
2 T. Carrington, *J. Chem. Phys., 41* (1964) 2021.
H. L. Snyder, B. T. Smith, T. P. Parr and R. M. Martin, *Chem. Phys., 65* (1982) 397.
3 L. Batt and R. T. Milne, *Int. J. Chem. Kinet., 9* (1977) 141.
4 C. A. F. Johnson, V. Freestone and J. Giovenacci, *J. Chem. Soc., Perkin Trans. II,* (1978) 584.
5 F. Lahmani, C. Lardeux, M. Lavollee and D. Solgadi, *J. Chem. Phys., 73* (1980) 1187, 4433.
6 D. D. Davies and W. Braun, *Appl. Opt., 7* (1968) 2071.
7 J. H. Koltz and D. W. Setser, in D. W. Setser (ed.), *Reactive Intermediates in the Gas Phase,* Academic Press, New York, 1979, p. 151.
8 V. E. Bondybey and T. A. Miller, *J. Chem. Phys., 66* (1977) 3337.
9 R. W. Nicholls, *J. Res. Natl. Bur. Stand., Sect. A, 68* (1964) 535.
10 L. T. Earls, *Phys. Rev., 48* (1935) 423.
11 R. Engleman, Jr., and P. E. Rouse, *J. Mol. Spectrosc., 37* (1971) 240.
12 C. Larrieu, A. Dargelos and M. Chaillet, *Chem. Phys. Lett., 91* (1982) 465.
13 E. H. Fink, *Habilitationschrift,* University of Bonn, 1976.
14 J. Kosanetzky, U. List, W. Urban, H. Vormann and E. H. Fink, *Chem. Phys., 50* (1980) 361.
15 I. M. Campbell and R. S. Mason, *J. Photochem., 8* (1978) 321.
16 I. M. Campbell and R. S. Mason, *J. Photochem., 8* (1978) 375.